Angewandte Chemie
Eine Zeitschrift der Gesellschaft Deutscher Chemiker

Supporting Information

Photoswitchable NIR-Emitting Gold Nanoparticles

*Sara Bonacchi, Andrea Cantelli, Giulia Battistelli, Gloria Guidetti, Matteo Calvaresi, Jeannette Manzi, Luca Gabrielli, Federico Ramadori, Alessandro Gambarin, Fabrizio Mancin, and Marco Montalti**

anie_201604290_sm_miscellaneous_information.pdf

Supporting Information

Photoswitchable NIR emitting gold nanoparticles

Sara Bonacchi,[a] Andrea Cantelli,[a] Giulia Battistelli,[a] Gloria Guidetti,[a] Matteo Calvaresi,[a] Jeannette Manzi,[a] Luca Gabrielli,[b] Federico Ramadori,[b] Alessandro Gambarin,[b] Fabrizio Mancin[b] and Marco Montalti[a]*

[a] Department of Chemistry "G. Ciamician", University of Bologna, Via Selmi 2, 40126, Bologna, Italy e-mail: marco.montalti2@unibo.it

[b] Department of Chemical Sciences Università degli Studi di Padova via Marzolo 1, 35131 Padova (Italy).

Table of Contents

1. Experimental Procedures.

General: Solvents were purified by standard methods. All commercially available reagents and substrates were used as received.

TLC analyses were performed using Merck 60 F_{254} precoated silica gel glass plates. Column chromatography was carried out on Macherey-Nagel silica gel 60 (70-230 mesh).

NMR spectra were recorded using a Bruker AV III 500 spectrometer operating at 500 MHz for ^{1}H, 125.8 MHz for ^{13}C. Chemical shifts are reported relative to internal Me4Si. Multiplicity is given as follow: s = singlet, d = doublet, t = triplet, q = quartet, qn = quintet, m = multiplet, br = broad peak.

HRMS mass spectra were obtained with an Mariner Applied Biosystem (API-TOF) mass spectrometer (MeOH, 0.5% formic acid).

Melting temperatures were measured using a Stuart SMP10 apparatus.

Elemental analysis were performed with a Perkin-Elmer 2400 CHN microanalyzer.

IR spectra were obtained using a Nicolet 5700 FT-IR spectrometer.

TEM images were recorded on a Jeol 300 PX electron microscope. One drop of sample was placed on the sample grid and the solvent was allowed to evaporate. UV-Visible spectra and kinetic traces were recorded on Cary 50 spectrophotometer equipped with thermostated multiple cell holders. Thermogravimetric analysis (TGA) was run on 1-2 mg nanoparticle samples using a Q5000 IR model TA instrument from 30 to 1000 °C under a continuous air flow.

2. Synthesis of 8-(4-((4-methoxyphenyl)diazenyl)phenoxy)octyl-thiol (*t*A)

The azobenzyl-thiol derivative ***t*A** has been prepared according to the following scheme:

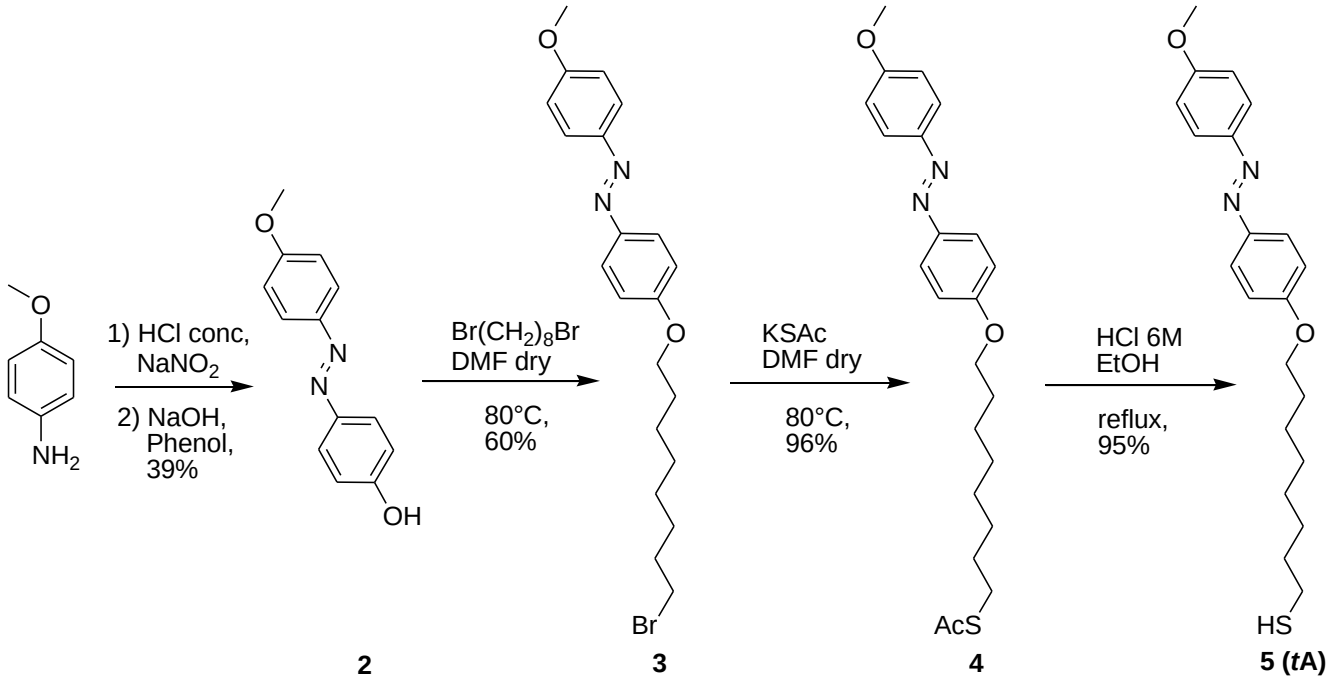

Scheme S1. Synthesis of the azobenzene derivative ***t*A**

2.1 Synthesis of 4-((4-methoxyphenyl)diazenyl)phenol (2)

1.6 g (12.993 mmol, 1 equiv) of *p*-anisidine are dissolved in 30 mL of milliQ water, then the solution is cooled to 0° C in an ice bath and 6 mL of concentrated HCl are added dropwise. Subsequently, 896 mg of $NaNO_2$ (12.993 mmol, 1 equiv) are added and the reaction is stirred for 1 h at 0°C . Then, 1.22 g of phenol (12.993 mmol, 1 equiv), dissolved in 20 mL of a 2.5 M NaOH solution in water, are added. The mixture is stirred for 15 minutes, then the precipitate is filtered off and washed with 5 mL of H_2O, obtaining 1.13 g (yield 39 %) of product **2**. Data are in agreement with those reported in literature.[1]

^{1}H NMR (500 MHz, MeOD) δ 7.83 (d, *J* = 9.0 Hz, 4H, H Ar), 7.78 (d, *J* = 8.8 Hz, 4H, H Ar), 7.04 (d, *J* = 9.0 Hz, 4H, H Ar), 6.92 (d, *J* = 8.8 Hz, 4H, H Ar), 3.87 (s, 3H, C*H*$_3$O).

^{13}C NMR (126 MHz, MeOD) δ 161.8 (1C, C_{quat} Ar), 160.2 (1C, C_{quat} Ar), 146.8 (1C, C_{quat} Ar), 146.0 (1C, C_{quat} Ar), 124.2 (1C, C Ar), 123.8 (1C, C Ar), 115.3 (1C, C Ar), 113.9 (1C, C Ar), 54.7(1C, *C*H$_3$O).

2.2 Synthesis 1-(4-((8-bromooctyl)oxy)phenyl)-2-(4-methoxyphenyl)diazene (3)

750 mg (3.286 mmol, 1 equiv) of compound **2** are dissolved in 5 mL of dry DMF, then 2.42 mL of 1,8-dibromoctane (13.144 mmol, 4 equiv) and 1.8 g of K_2CO_3 (13.144 mmol, 4 equiv) are added. The mixture is stirred under N_2 at 80°C for 5 hours. The solvent is then removed by evaporation at reduced pressure and the reaction crude is extracted in DCM/H_2O; the organic phases are collected, dried over Na_2SO_4 and the solvent is removed under reduced pressure. Purification by flash chromatography (Exane : DCM from 5:5 to 4:6), gives 825 mg (60% yield) of product **3**.

^{1}H NMR (500 MHz, $CDCl_3$) δ 7.94 – 7.87 (m, 4H, H Ar), 7.06 – 6.99 (m, 4H, H Ar), 4.06 (t, *J* = 6.5 Hz, 2H, C*H*$_2$OPh), 3.91 (s, 2H, C*H*$_3$O), 3.44 (t, *J* = 6.8 Hz, 2H, C*H*$_2$Br), 1.94 – 1.87 (m, 2H, CH_2), 1.87 – 1.79 (m, 2H, CH_2), 1.55 – 1.45 (m, 4H, CH_2), 1.44 – 1.36 (m, 4H, CH_2).

^{13}C NMR (126 MHz, $CDCl_3$) δ 161.6 (1C, C_{quat} Ar), 161.2 (1C, C_{quat} Ar), 147.0 (1C, C_{quat} Ar), 146.9 (1C, C_{quat} Ar), 124.4 (1C, C Ar), 124.4 (1C, C Ar), 114.7 (1C, C Ar), 114.2 (1C, C Ar), 68.2 (1C, *C*H$_2$OPh), 55.6 (1C, *C*H$_3$O), 34.0 (1C, *C*H$_2$Br), 32.8 (1C, *C*H$_2$), 29.2(1C, *C*H$_2$), 28.7(1C, *C*H$_2$), 28.1 (1C, *C*H$_2$), 25.9 (1C, *C*H$_2$).

TOF ES$^+$ HRMS: [M+H$^+$] calcd. for $C_{21}H_{28}BrN_2O_2$ = 419.1329. Found = 419.1320.

IR ν (KBr): 2941, 1601, 1581, 1500, 1249, 1146, 844, 548 cm^{-1}.

Melting Point: 98÷99°C

Elemental anal. Calcd for $C_{21}H_{27}BrN_2O_2$ = C, 60.27; H, 6.51; N, 6.70. Found = C, 60.52; H, 6.52; N, 6.70.

2.3 Synthesis of 8-(4-((4-methoxyphenyl)diazenyl)phenoxy)octyl)thioacetate (4)

Compund **3** (710 mg, 1.693 mmol, 1 equiv) is dissolved in 8 mL of dry DMF, then potassium thioacetate (580 mg, 5.079 mmol, 3 equiv) is added. The reaction mixture is stirred at 80°C under N_2 atmosphere for 4 hours. Then the solvent is removed by evaporation at reduced pressure and the residue is purified by flash chromatography (Exane : DCM from 5:5 to 100% DCM) obtaining 670 mg (96% of yield) of product **4**.

^{1}H NMR (500 MHz, $CDCl_3$) δ 7.93 – 7.87 (m, 4H, H Ar), 7.02 (dd, *J* = 8.8, 7.8 Hz, 4H, H Ar), 4.05 (t, *J* = 6.5 Hz, 2H, C*H*$_2$OPh), 3.90 (s, 3H, C*H*$_3$O), 2.90 (t, *J* = 7.3 Hz, 2H, C*H*$_2$S), 2.35 (s, 3H, C*H*$_3$COS), 1.89 – 1.79 (m, 2H, C*H*$_2$), 1.64 – 1.55 (m, 2H, C*H*$_2$), 1.53 – 1.44 (m, 2H, C*H*$_2$), 1.45 – 1.32 (m, 6H, C*H*$_2$).

^{13}C NMR (126 MHz, $CDCl_3$) δ 196.06 (1C, CH_3*C*OS), 161.5 (1C, C_{quat} Ar), 161.2 (1C, C_{quat} Ar), 147.1 (1C, C_{quat} Ar), 146.9 (1C, C_{quat} Ar), 124.4 (1C, C Ar), 124.3 (1C, C Ar), 114.7 (1C, C Ar), 114.2 (1C, C Ar), 68.3 (1C, *C*H_2OPh), 55.6 (1C, *C*H_3O), 30.7 (1C, *C*H_2S), 29.5(1C, *C*H_2), 29.2 (1C, *C*H_2), 29.2 (1C, *C*H_2), 29.1 (1C, *C*H_2), 29.0 (1C, *C*H_2), 28.7 (1C, *C*H_2), 25.9 (1C, *C*H_2).

TOF ES$^+$ HRMS: [M+H$^+$] calcd. for $C_{23}H_{31}N_2O_3S$ = 415.2050. Found = 415.2032.

IR: ν (KBr): 2927, 1683, 1601, 1581, 1248, 1121, 1106 cm^{-1}.

Melting Point: 106÷107°C

Elemental anal. Calcd for $C_{23}H_{30}N_2O_3S$ = C, 66.64; H, 7.29; N, 6.76; S, 7.73. Found = C, 66.51; H, 7.66; N, 6.66; S, 7.76.

2.4 Synthesis of 8-(4-((4-methoxyphenyl)diazenyl)phenoxy)octyl)thiol (5/*t*A)

Compound **4** (200 mg, 0.482 mmol) is suspended in 8 mL of a EtOH : HCl 6M 1:1 mixture, and the reaction is refluxed under N_2 atmosphere for 3 hours. Then the solvent is evaporated under reduced pressure and subsequent purification by flash chromatography (100% DCM) gives the final thiol **5** (170 mg, 95% yield)

^{1}H NMR (500 MHz, $CDCl_3$) δ 7.96 – 7.90 (m, 4H, H Ar), 7.06 – 6.99 (m, 4H, H Ar), 4.06 (t, *J* = 6.5 Hz, 2H, C*H*$_2$OPh), 3.91 (s, 3H, OC*H*$_3$), 2.56 (dd, *J* = 14.7, 7.5 Hz, 2H, C*H*$_2$S), 1.88 – 1.80 (m, 2H, C*H*$_2$), 1.68 – 1.60 (m, 2H, C*H*$_2$), 1.54 – 1.47 (m, 2H, C*H*$_2$), 1.46 – 1.31 (m, 6H, C*H*$_2$).

^{13}C NMR (126 MHz, $CDCl_3$) δ 161.8 (1C, C_{quat} Ar), 161.4 (1C, C_{quat} Ar), 146.6 (1C, C_{quat} Ar), 146.5 (1C, C_{quat} Ar), 124.6 (1C, C Ar), 124.5 (1C, C Ar), 114.8 (1C, C Ar), 114.3 (1C, C Ar), 68.3 (1C, *C*H_2OPh), 55.6 (1C, *C*H_3O), 34.0 (1C, *C*H_2SH), 29.3 (1C, *C*H_2), 29.2 (1C, *C*H_2), 29.0 (1C, *C*H_2), 28.3 (1C, *C*H_2), 26.00 (1C, *C*H_2), 24.6 (1C, *C*H_2).

TOF ES$^+$ HRMS: [M+H$^+$] calcd. for $C_{21}H_{29}N_2O_2S$ = 373.1944. Found = 373.1960.

IR: ν (KBr): 2924, 1601, 1582, 1501, 1246, 1147, 1021, 849 cm^{-1}.

Melting Point: 93÷94°C

Elemental anal. Calcd for $C_{21}H_{28}N_2O_2S$ = C, 67.71; H, 7.58; N, 7.52; S, 8.61. Found = C, 67.68; H, 8.05; N, 7.25; S, 8.36.

3. Synthesis and characterization of monolayer protected gold nanoparticles (*t*A-GNPs)

Monolayer protected gold nanoparticles (***t*A-GNPs**) were prepared according to a previously reported two-step procedure. [2]All the glassware used in the ***t*A-GNPs** preparation was washed with aqua regia and rinsed with distilled water. $HAuCl_4$ is strongly hygroscopic and was weighted within a dry-box.

A solution of $HAuCl_4 \cdot 3H_2O$ (100 mg, 0.254 mmol) in water (4 mL) was extracted with a solution of tetraoctylammonium bromide (5 g, 9.14 mmol) in N_2 purged toluene (250 mL). To the resulting reddish-orange organic solution, dioctylamine (3.36 g, 13.92 mmol) is added (the amount of dioctylamine was calculated[2] in order to obtain 2 nm nanoparticles). The mixture is vigorously stirred under N_2 for 30 min. During this period of time the color of the mixture fades. A solution of $NaBH_4$ (93.0 mg, 2.46 mmol) in H_2O (1 mL) is then rapidly added. The color of the solution turns rapidly to black due to nanoparticles formation. After 2 hours of stirring, the aqueous layer is removed. To the above nanoparticle solution, thiol ***t*A** (0.254 mmol) dissolved in 3 mL of isopropanol is rapidly added. The reaction mixture is evaporated and the resulting crude is dissolved in CH_2Cl_2 and purified by gel permeation chromatography with Biorad Bio-Beads S-X1 resin.

3.1. Characterization of *t*A-GNPs

TEM analysis of the different samples of small nanoparticles (Figure S1) yields an average diameter for the MPGN of 1.7±0.6 nm.

Formula for ***t*A-GNPs** calculate on the basis of TEM diameter and TGA analysis is $Au_{152}RS_{62}$, in agreement with the well-known $Au_{144}RS_{60}$ nanocluster which likely constitutes the majority of the nanoparticles in the sample.[3] TGA analysis of a sample of ***t*A-GNPs** under air atmosphere is shown in

Figure S2. NMR analysis (Figure S3) indicates monolayer formation (broadening of all signals), as confirmed by diffusion-filtered experiments (not shown).

UV-Vis spectrum of figure 1 (main text) confirms the GNPs composition. The spectrum was recorded for a solution prepared by dissolving 0.9 mg ***t*A-GNPs** in 50 ml of $CHCl_3$ ($c_{tA\text{-}GNP}$ = 18 μg ml^{-1}). The concentration of ***tA*** in the solution was hence calculated according to the Lambert-Berr law A = εbc (where A is the absorbance, ε is the molar absorption coefficient, c is the concentration and b = 1 cm is the optical path) to be $2.2x10^{-5}$ M and hence 8 μg ml^{-1}. The gold concentration was hence 10 μg ml^{-1} corresponding to 5.0 $x10^{-5}$M. The molar Au/ligand ratio was hence 2.3 (2.4 expected for Au_{144}***tA***$_{60}$). Moreover the absorption at 510 nm is consistent with the reported molar absorption coefficient for Au_{144} (ε_{510}=$4.34x10^{-5}$ M)[4] being the molecular weight of Au_{144}***tA***$_{60}$ MW= 50756 g/mol.

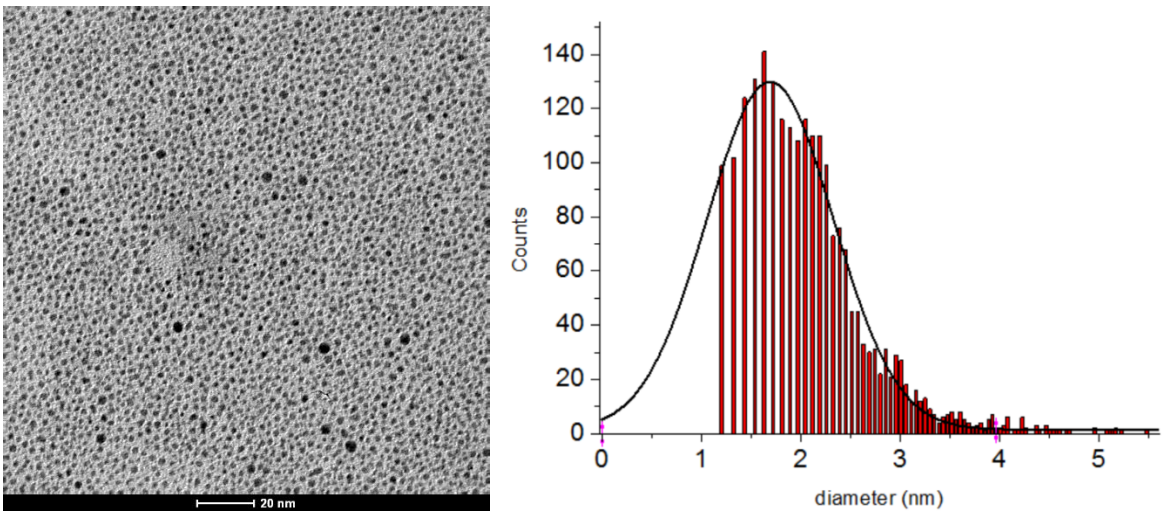

Figure S1: Sample TEM image of ***t*A-GNPs** and size distribution: average diameter = 1.7 nm (σ= 0.6 nm).

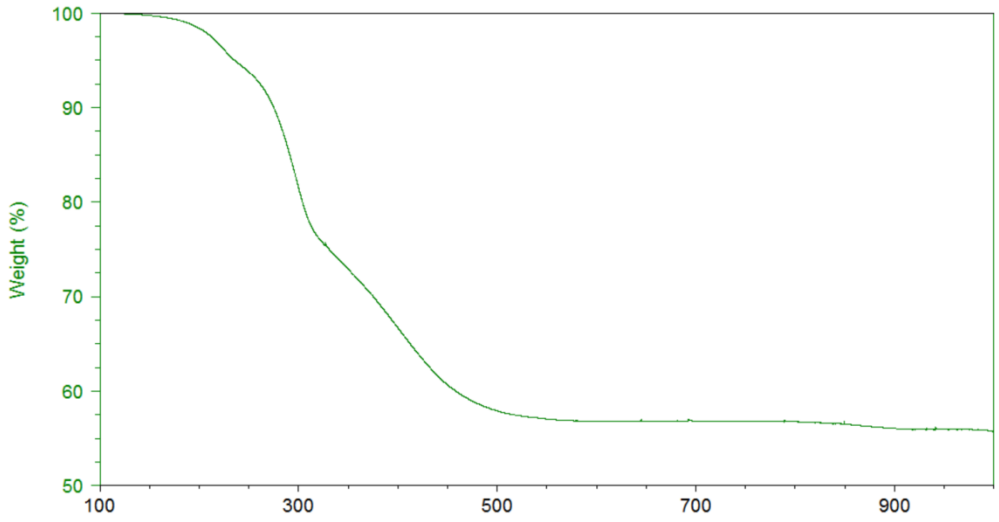

Figure S2: TGA analysis of a sample of ***t*A-GNPs** under air atmosphere.

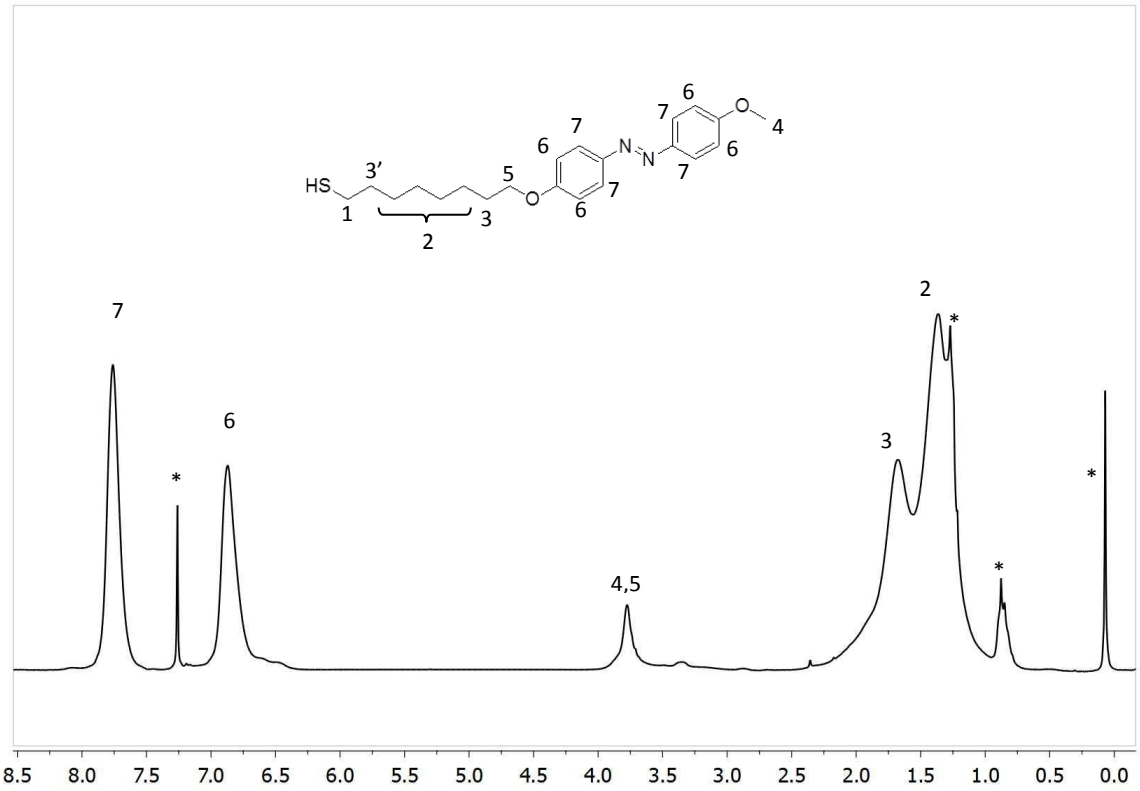

Figure S3: ^{1}H-NMR (300 MHz) spectrum of the ***t*A-GNPs** in $CDCl_3$ (* indicates the residual solvents and impurities). Signals from methylenes 1 and 3' are likely undetectable due to strong line broadening due to their closeness to nanoparticle surface.

4. Photophysical measurements.

All photophysical measurement were performed in air-equilibrated chloroform solution (Merk Uvasol) UV-VIS absorption spectra were performed at 298 K by means of Perkin-Elmer Lambda 45 spectrophotometer. Quartz cuvette with optical path length of 1 cm were used (Hellma). The estimated experimental errors are: 2 nm on the band maximum, 5% on the molar absorption coefficient.

The luminescence spectra were recorded with a spectrofluorimeter Edinburgh FLS920 equipped with a photomultiplier Hamamatsu R928P for the visible region and a a Ge detector for emission in the NIR spectral region. Correction of the emission spectra for detector sensitivity in the 700−1200 nm spectral region was performed.[5]

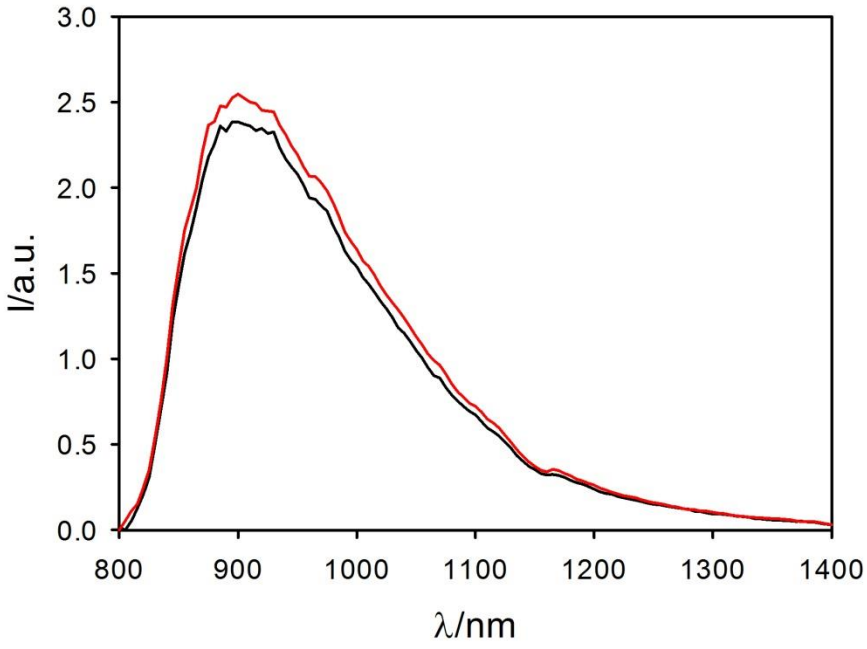

Figure S4 Luminescence spectra (λ_{exc}=550 nm) of the thermodynamically stable ***t*A-GNP** in $CHCl_3$ (red line) and of the photo-isomerized NPs ***c*A-GNP** (black).

5. Photoisomerization experiments.

Photochemical experiments were performed in air-equilibrated chloroform solution (Merk Uvasol). Irradiation at 360 and 480 nm were performed in a spectrofluorimeter Edinburgh FLS920 equipped with a 450 W Xenon lamp. Irradiation wavelength was selected by positioning the excitation monochromator and using 10 nm band-pass slits. The irradiated solution was contained in a spectrophotometric cell (1 cm or 0.3 cm path) and magnetically stirred continuously. The intensity of the incident photon flux was measured by the ferrioxalate actinometer. [5]

The estimated experimental errors are: 10% on the photoreaction quantum yield, 5% on the composition of the photostationary state.

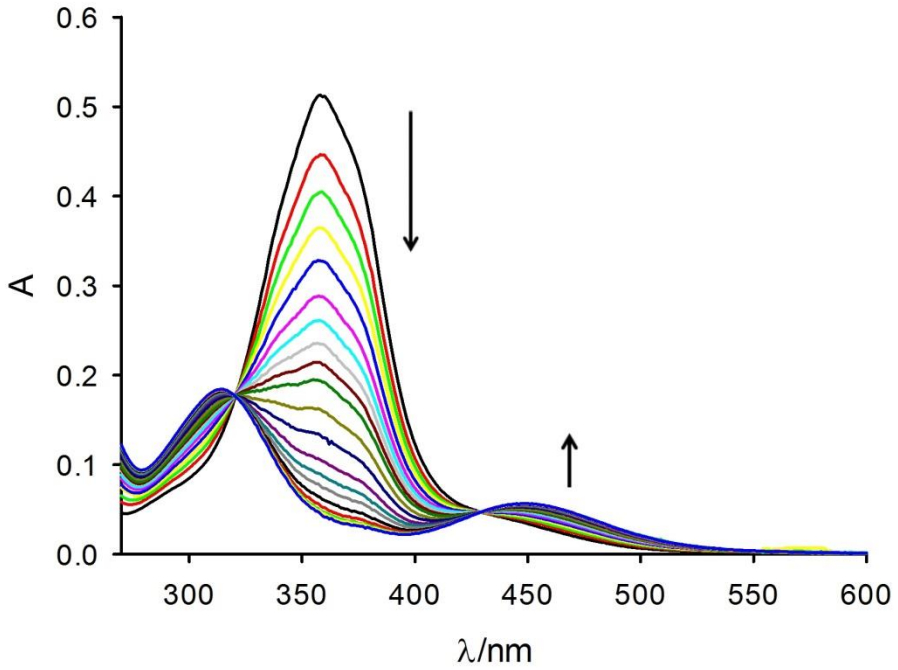

Figure S5 Absorption spectra of a $2x10^{-5}$M solution of ***t*A** in $CHCl_3$ during irradiation at 360 nm.

6. Photoisomerization kinetic model

The trans azobenzene (T) photo-isomerization[6] quantum yield $\phi_T$is the ratio between the number of isomerized T molecules per time unit and the number of photons adsorbed by T per time unit. [5]

$$\phi_T = \frac{-d[T]}{I_0 f_T dt} V$$

[Eq. 1]

Where I_0Is the number of incident photon for time unit, f_T is the fraction of incident photon absorbed by T and V is the solution volume. Photoisomerization of T produces the cis form (C) according to the process:

$$T^* \rightarrow C$$

If irradiation wavelength is suitable to excite the produced C its photoisomerization occours according to the process:

$$C^* \rightarrow T$$

The C photo-isomerization quantum yield $\phi_C$is defined analogously to the one of T:

$$\phi_C = \frac{-d[C]}{I_0 f_C dt} V$$

[Eq. 2]

Where f_T is the fraction of incident photon absorbed by C.

In general for a solution containing i species the fraction of light absorbed by each species f_i can be calculated knowing its contribution A_i, to the absorbance A or its molar absorption coefficient ε_i and the optical path b:

$$A = \sum_i A_i = \sum_i b\varepsilon_i[i]$$

$$f_i = \frac{1 - 10^{-A}}{A} A_i = \frac{1 - 10^{-A}}{A} b\varepsilon_i[i]$$

[Eq. 3]

Considering that in the absence of other photochemical process:

$$[T] + [C] = cost = c_0$$

and hence:

$$\frac{d[T]}{dt} = \frac{-d[C]}{dt}$$

The combination of Eq. 1, 2 and 3 gives the following isomerization rate equation: [5]

$$\frac{d[C]}{dt} = \frac{bI_0}{V}\frac{(1-10^{-A})}{A}\phi_T\varepsilon_T(c_0 - [C]) - \frac{bI_0}{V}\frac{(1-10^{-A})}{A}\phi_c\varepsilon_C[C]$$

[Eq. 4]

At the photostationary state (reached at $t \to \infty$) $[C] = [C]_\infty$ and $d[C]/dt = 0$, hence:

$$\phi_c = \frac{\varepsilon_T(c_0 - [C]_\infty)}{\varepsilon_C[C]_\infty}\phi_T$$

Which can be replaced in eq. 4 giving:

$$\frac{d[C]}{dt} = \frac{bI_0}{V}\frac{(1-10^{-A})}{A}\phi_T\varepsilon_T c_0(1 - \frac{[C]}{[C]_\infty})$$

[Eq. 5]

As far as the absorbance is concerned, for the azobenzene functionalized GNP where the contribution of the gold to the total absorbance is A_G becomes:

$$A = \varepsilon_T b(c_0 - [C]) + \varepsilon_C b[C] + A_G = b(\varepsilon_C - \varepsilon_T)[C] + \varepsilon_T b c_0 + A_G$$

$$A = b(\varepsilon_C - \varepsilon_T)[C] + A_0$$

And hence:

$$[C] = \frac{A - A_0}{b(\varepsilon_C - \varepsilon_T)} \; ; \; \frac{d[C]}{dt} = \frac{1}{b(\varepsilon_C - \varepsilon_T)}\frac{dA}{dt}$$

[Eq. 6]

The combination of Eq. 5 and Eq. 6 gives:

$$\frac{dA}{dt} = \frac{I_0}{V}\frac{(1-10^{-A})}{A}\phi_T\varepsilon_T c_0[b(\varepsilon_C - \varepsilon_T) - \frac{A - A_0}{[C]_\infty}]$$

[Eq. 7]

At the photostationary state (reached at $t \to \infty$) $dA/dt = 0$

$$b(\varepsilon_C - \varepsilon_T) = \frac{A_\infty - A_0}{[C]_\infty}$$

And hence assuming $y_\infty = [C]_\infty / c_0$ Eq. 7 becomes:

$$\frac{dA}{dt} = -\frac{I_0}{V}\frac{(1-10^{-A})}{Ay_\infty}\phi_T\varepsilon_T(A - A_\infty)$$

[Eq. 8]

Which can be integrated to give:

$$ln\frac{A - A_\infty}{A_\infty - A_0} = -\frac{I_0}{Vy_\infty}\phi_T\varepsilon_T\int_0^t \frac{(1-10^{-A})}{A}dt$$

Defining:

$$x = \int_0^t \frac{(1-10^{-A})}{A}dt; B = \frac{I_0}{Vy_\infty}\varepsilon_T$$

[Eq. 9]

Equation 8 becomes:

$$ln\frac{A - A_\infty}{A_\infty - A_0} = -B\phi_T x$$

[Eq. 10]

The variable x was integrated numerically; all the factors composing the term B where known (I_0 was measured by the ferrioxalate actinometer). [5]

The linear fitting of the experimental data $ln\frac{A-A_\infty}{A_\infty-A_0}$ shown in figure S5 allowed us to determine ϕ_T

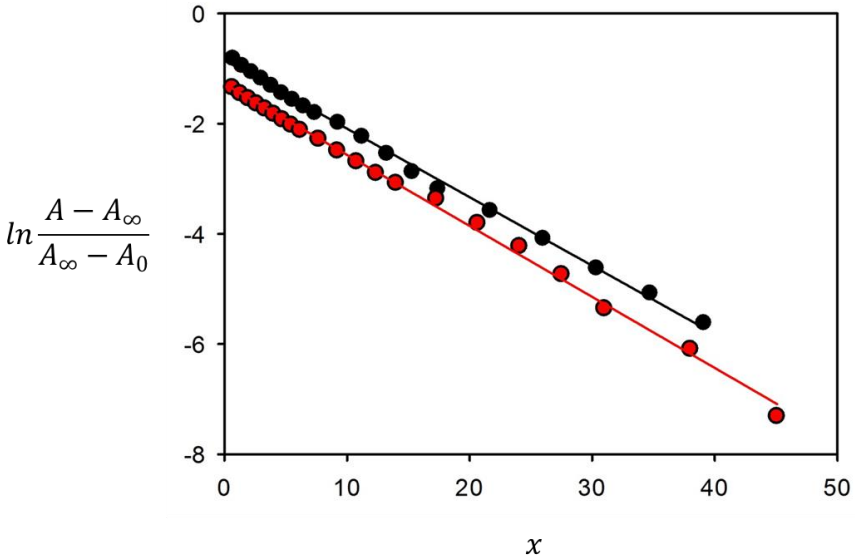

Figure S6 Linear fitting of the absorbance at λ=360 nm as a function of the coordinate x of equation 9 for the azobenzene derivative tA (black dots) and for the functionalized NPs (red dots). The fitting results were used to calculate the $\phi_T$values reported in the main article according to eq. 10.

7. ^{1}H, ^{13}C-NMR and IR and HRMS spectra of the synthesized compounds

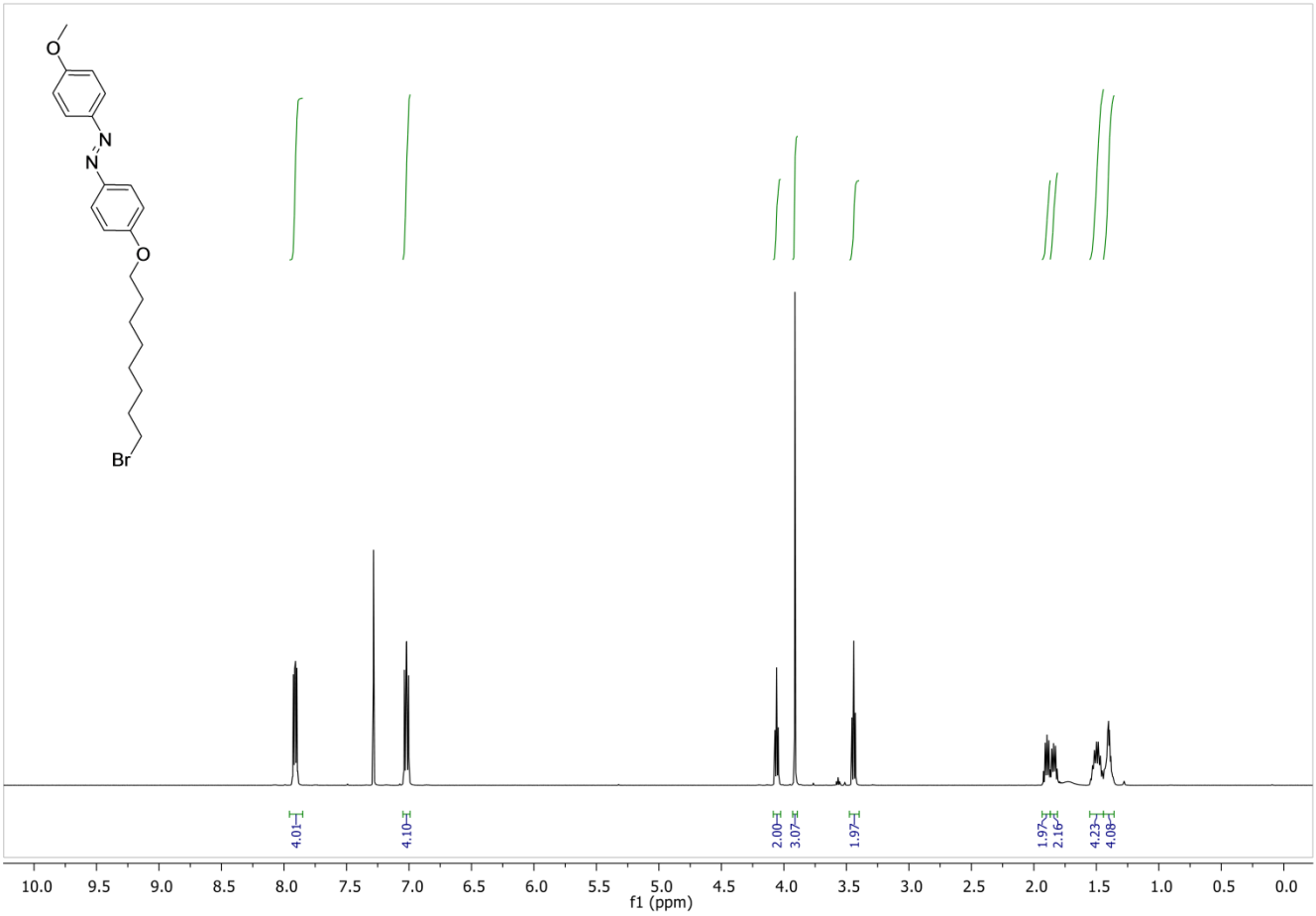

Figure S7 ^{1}H-NMR spectra of compound **3** ($CDCl_3$).

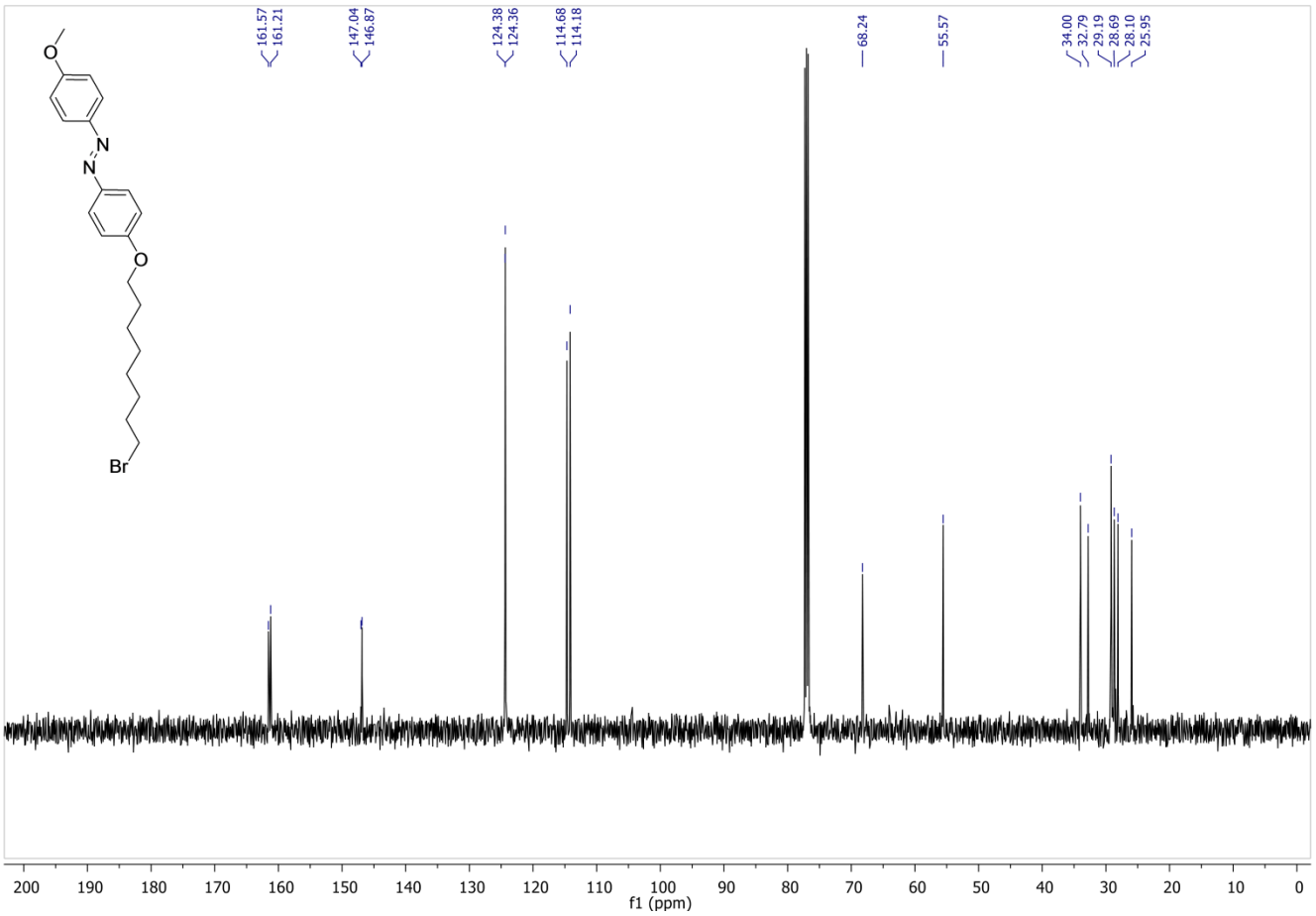

Figure S8 ^{13}C-NMR spectra of compound **3** ($CDCl_3$).

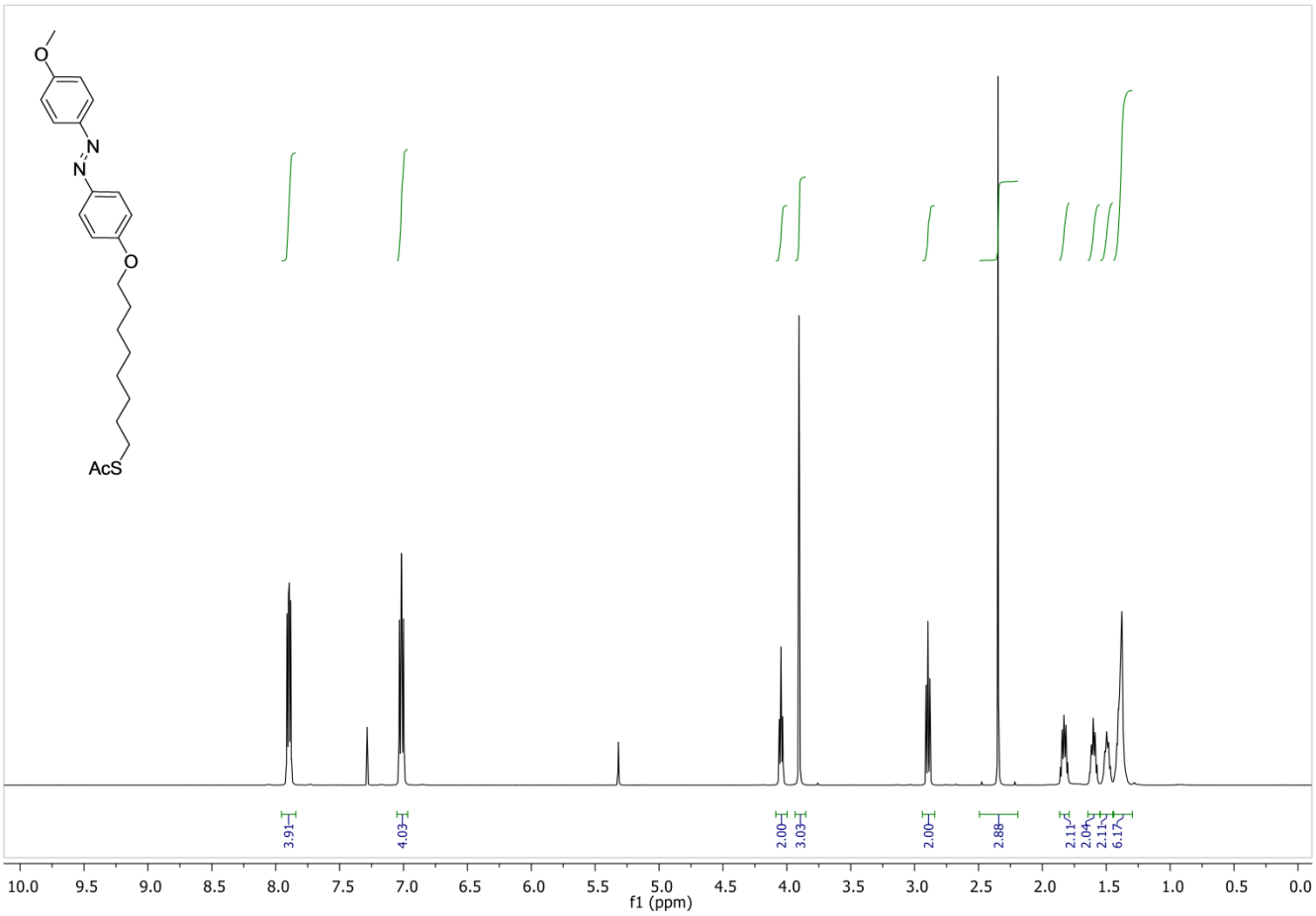

Figure S9 ^{1}H-NMR spectra of compound **4** ($CDCl_3$).

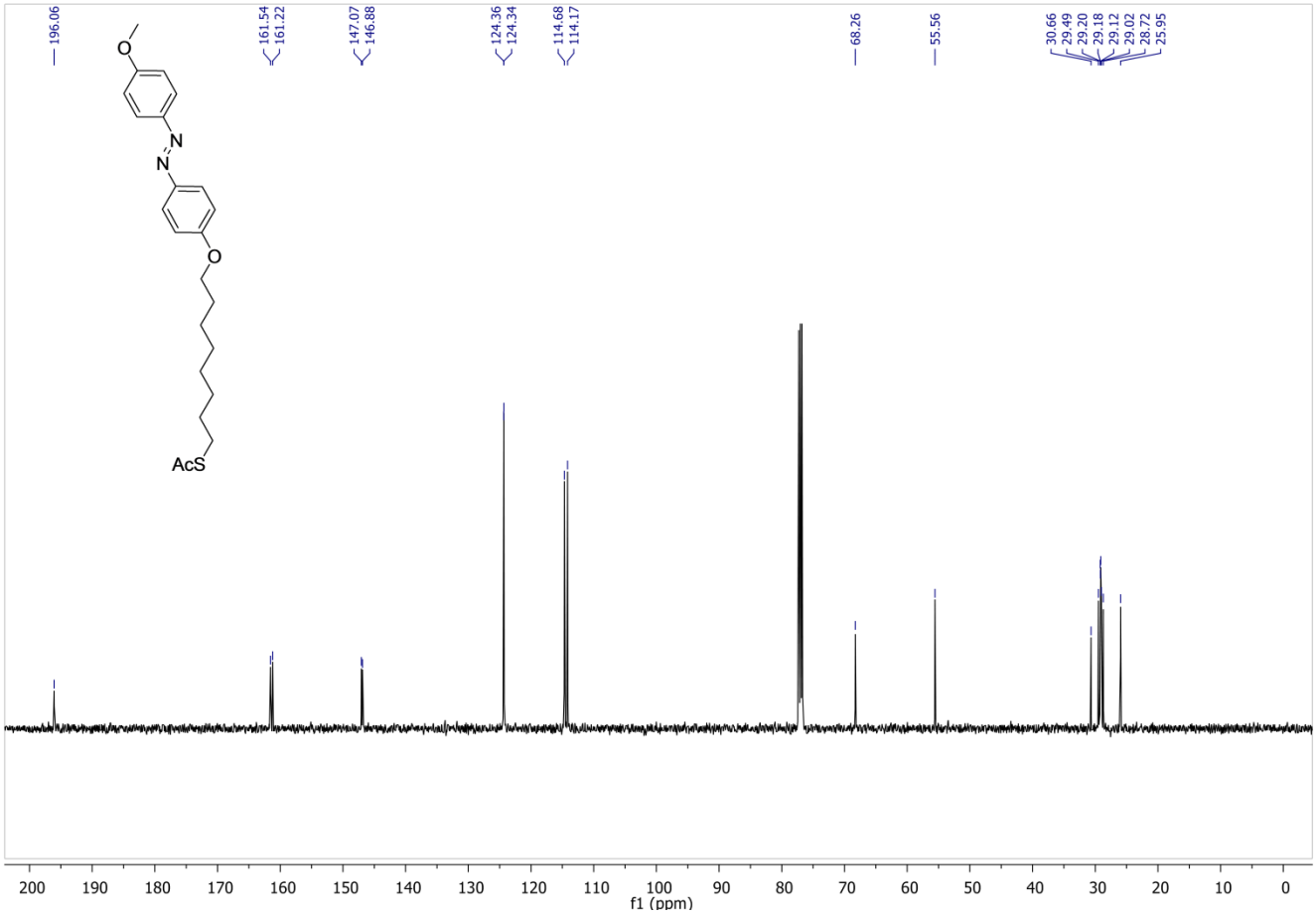

Figure S10 ^{13}C-NMR spectra of compound **4** ($CDCl_3$).

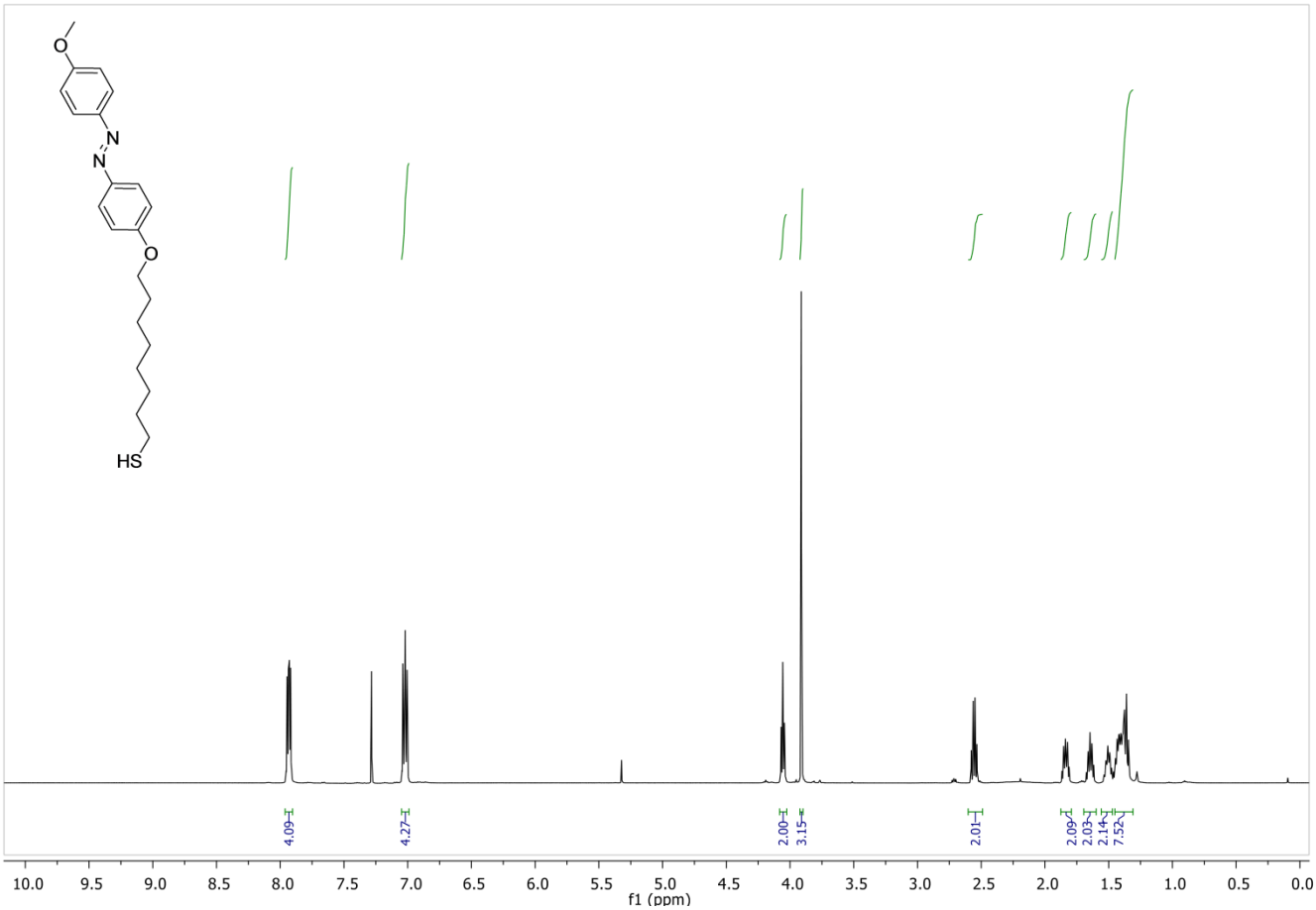

Figure S11 ^{1}H-NMR spectra of compound **5** ($CDCl_3$).

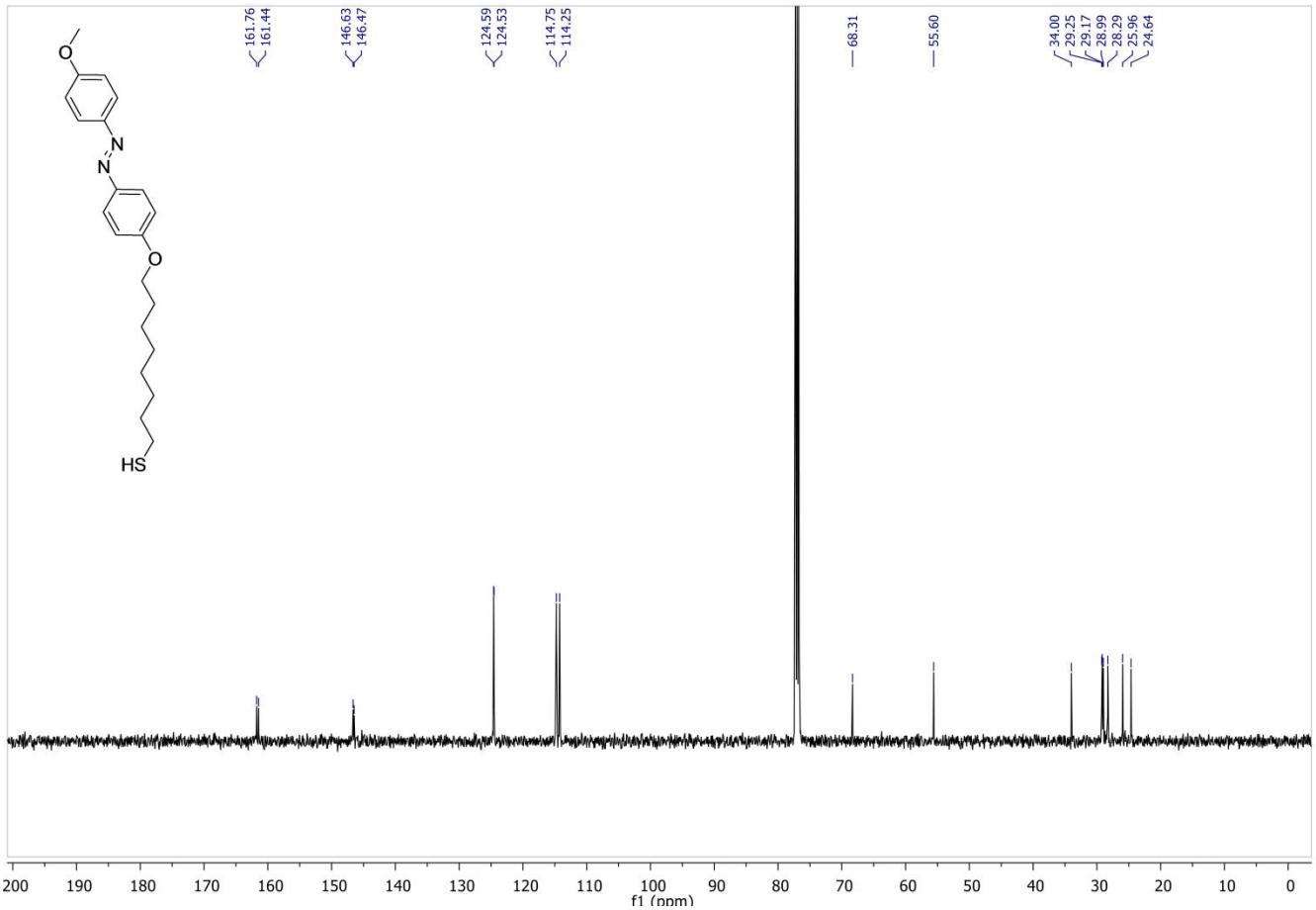

Figure S12 ^{13}C-NMR spectra of compound **5** ($CDCl_3$).

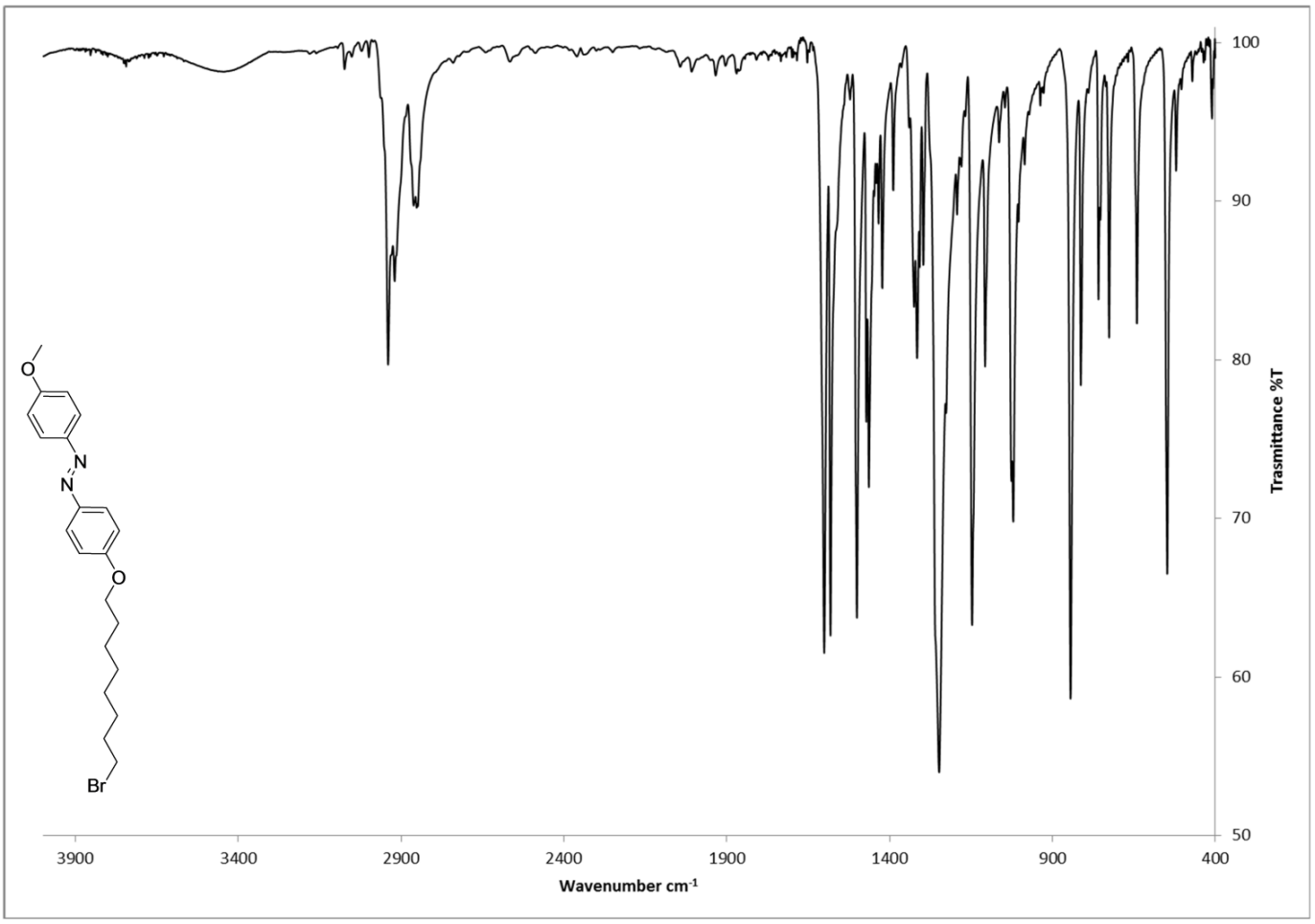

Figure S13 IR spectra of compound **3** (KBr).

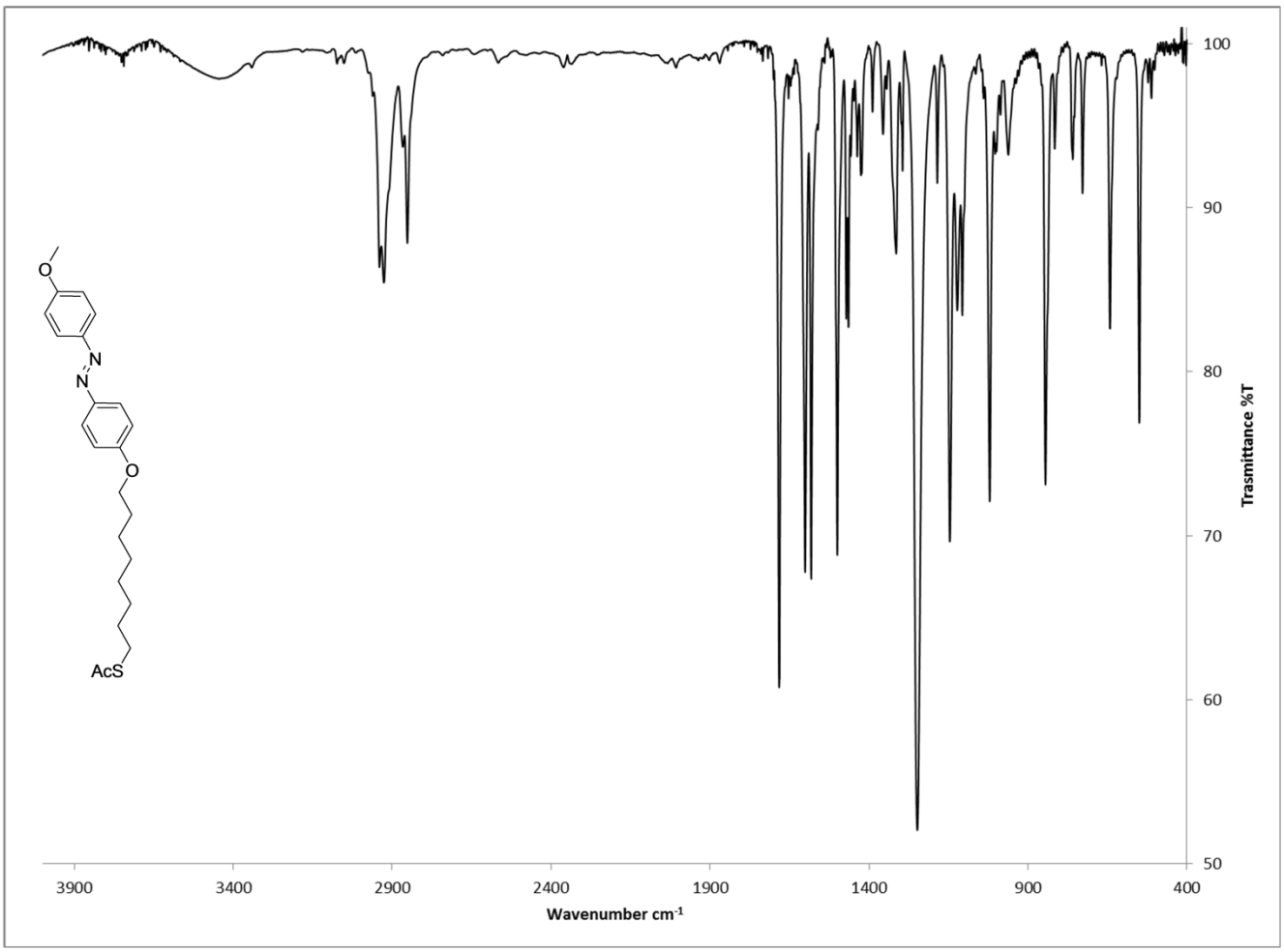

Figure S14 IR spectra of compound **4** (KBr).

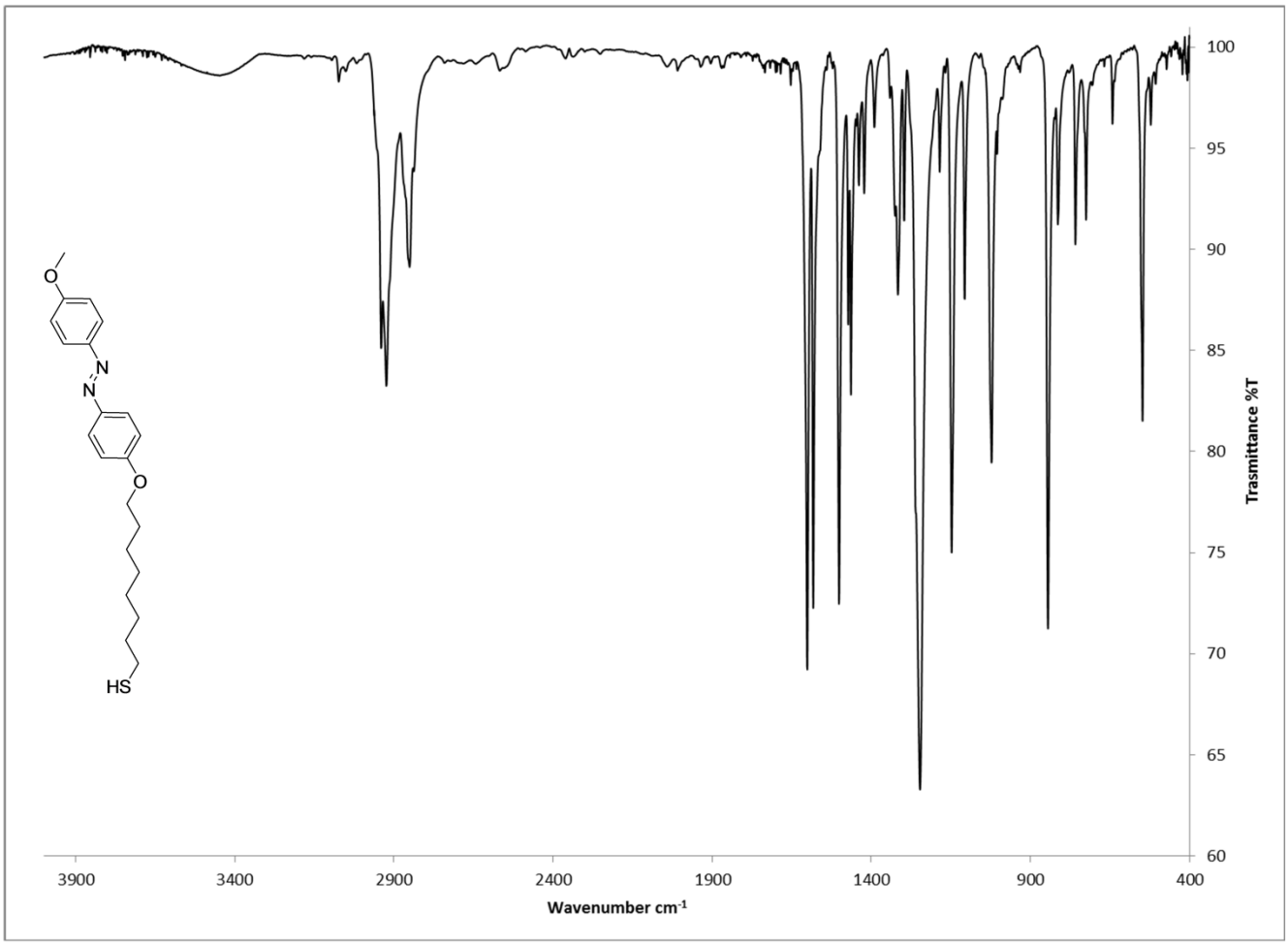

Figure S15 IR spectra of compound **5/*t*A** (KBr).

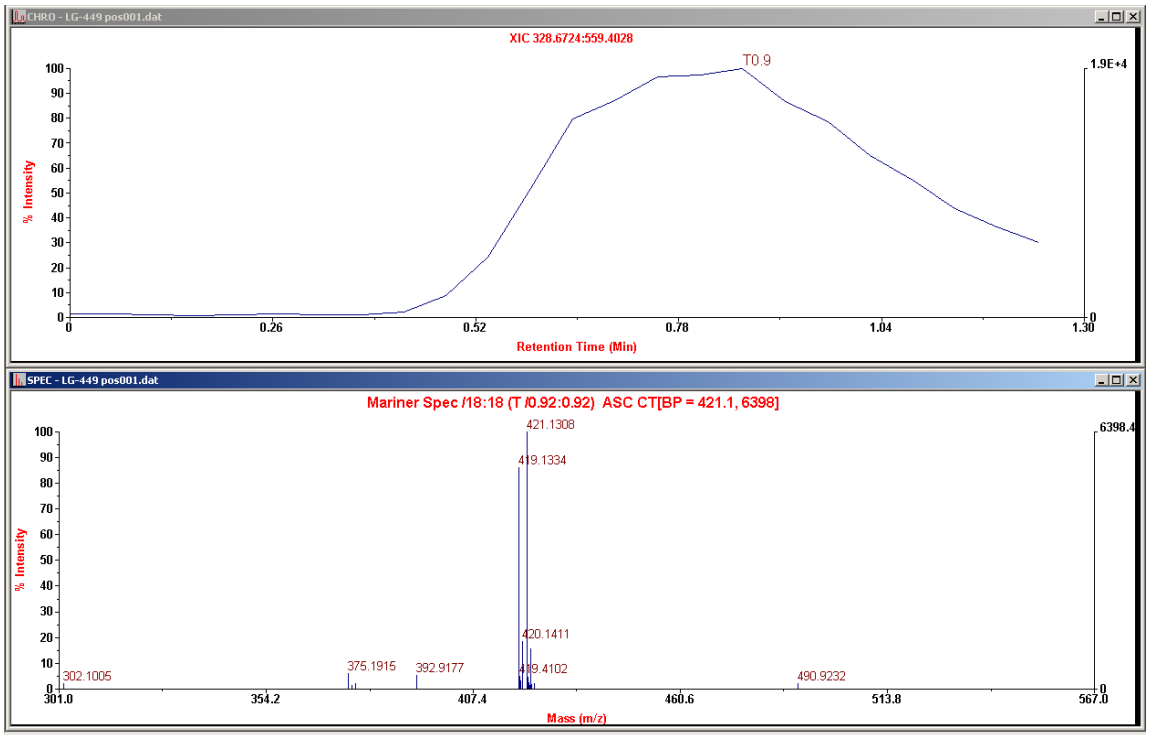

Figure S16 HRMS spectra of compound **3**.

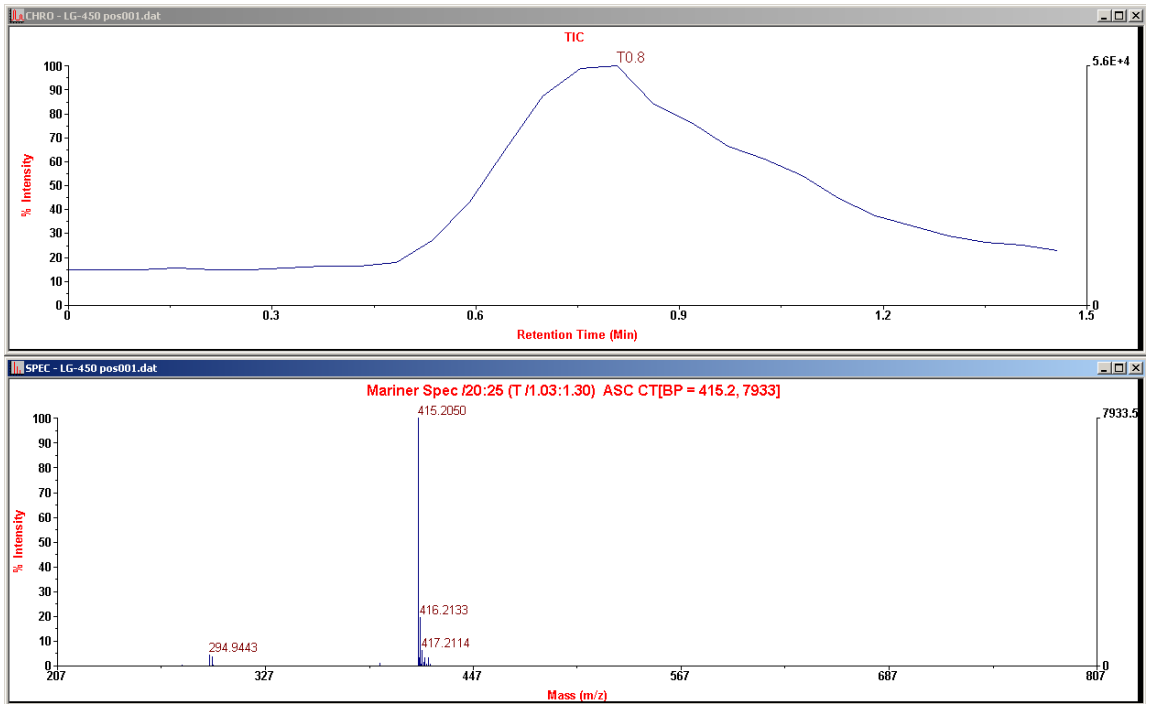

Figure S17 HRMS spectra of compound **4**.

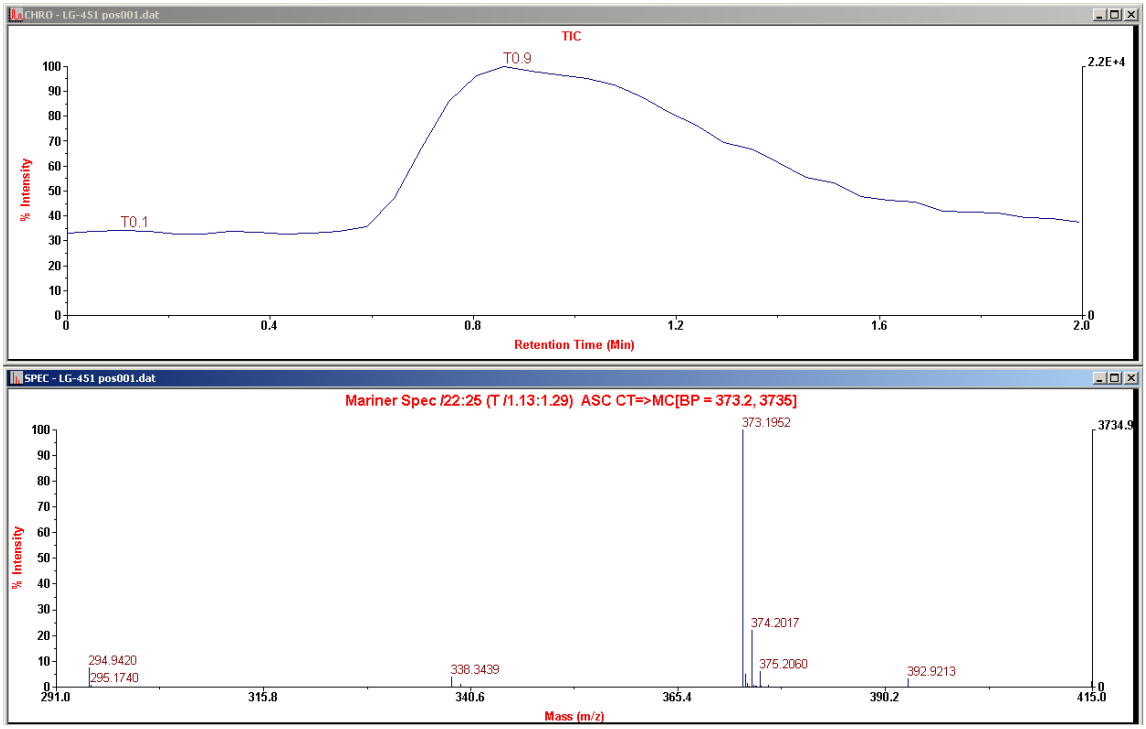

Figure S18 HRMS spectra of compound **5/*t*A**.

8 MD simulations: computational details

Parametrization. Thiolate-protected gold clusters are described using the recently developed unified AMBER-compatible molecular mechanics force field for thiolate-protected gold nanoclusters.[7]

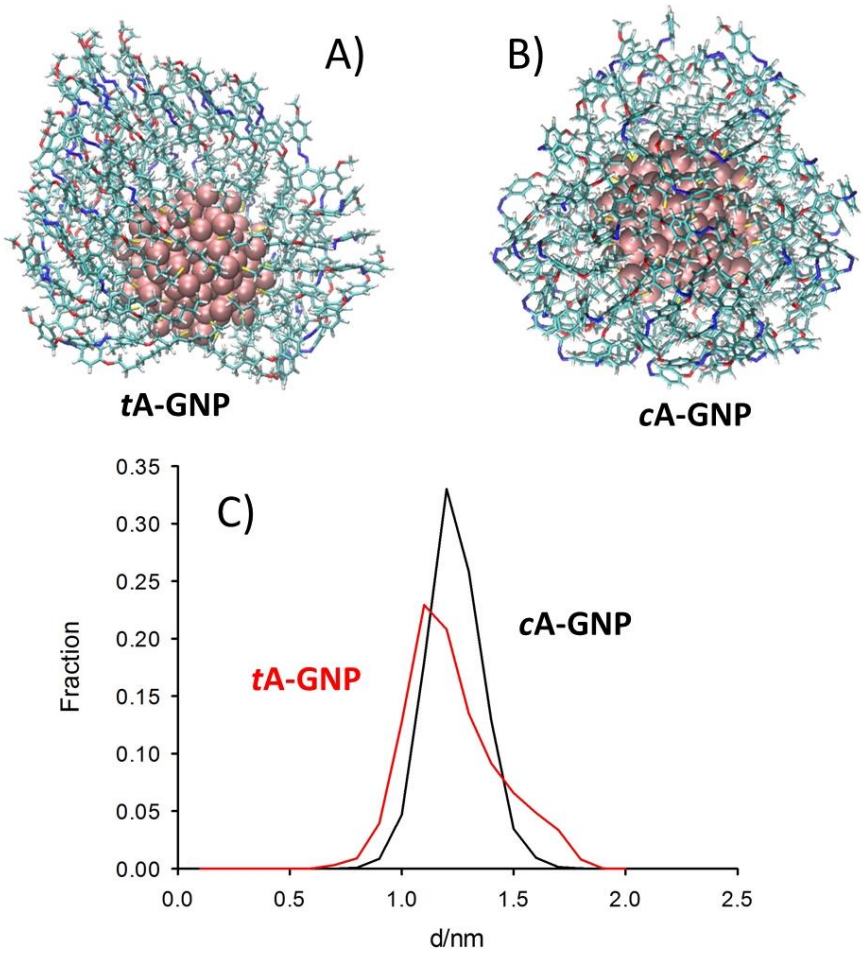

Figure S19 Atomic configuration taken from the last snapshot of MD simulation of A) hair brushed ***t*A-GNP**; B) hair ruffled ***c*A-GNP**; C) normalized radial distribution function averaged over the simulation time of the center of mass of the azobenzene moieties around the gold nanoparticles for ***t*A-GNP** (red line) and ***c*A-GNP** (black line).

The ligand parameters are described using the GAFF force field,[8] the partial charges on the ligand atoms (the S atom was capped by a hydrogen) were optimized following the RESP charge fitting procedure recommended for AMBER. [9] Modified GAFF parameters are used to described correctly the azobenzene *cis* and *trans* geometries.[10]

Geometries. The coordinates of the $Au144(SR)_{60}$ are taken from Ref. [11] and downloaded by Aalto University.[12] The methylthiolates (R=Me) are substituted by the 8-(4-((4-methoxyphenyl)diazenyl)phenoxy)octyl)thiol ligands (compound 5) described in this paper. Two systems are set-up, where the ligands are arranged radially respect to the gold nanoparticle surface, with the same linear alkyl chain geometries, but different *cis*/*trans* configuration of the azobenzene moieties. The thiolate-protected gold clusters are then immersed in a pre-equilbrated chloroform simulation box.

Simulation protocol. About 1000 steps of steepest descent minimization were performed with SANDER. The minimized structure (only cleared from severe sterical clashes) was considered for a 3 step equilibration protocol. Particle Mesh Ewald summation was used throughout (cut off radius of 10 Å for the direct space sum). Individual equilibration steps included

(i) 50 ps of heating to 298 K within an NVT ensemble.

(ii) 50 ps of equilibration MD at 298 K to switch from NVT to NPT and adjust the simulation box. Isotropic position scaling was used at default conditions.

(iii) 400 ps of continued equilibration MD at 298 K for an NPT ensemble

A production MD, with simulation conditions identical to the final equilibration step (iii), was then carried out. Overall sampling time was 50 ns.

Analysis of the trajectory. Using the ptraj module the radial distribution function is calculated over the simulation time. The centers of mass of the azobenzene moieties around the gold nanoparticles for ligands in *trans* and *cis* conformations are considered

9. Energy-tranfer models

Different models have been proposed for energy transfer from a molecular donor to gold NPs.[13] Nevertheless, as a general approach, the ET efficiency (η_{ET}) depends on the distance d and on a critical distance d_0 (which is characteristic of the donor-acceptor pair) according to the equation:

$$\eta_{ET} = 1 - \frac{1}{1 + (\frac{d_0}{d})^n}$$

[Eq. 11]

The exponent *n* changes according to the different theories being *n*=6 for the Forster Resonance Energy Transfer (FRET) model and *n*=4 for the Nano-Surface Energy Transfer (NSET) model.[13a] Other values for *n* has been experimentally determined in the case of GNP used as ET acceptor.[13b] According to Eq. 11, $\eta_{ET} = 0.5$ when $d = d_0$.

As discussed in the main text, independently from the ET model, according to Eq. 11, an increase of d, (as demonstrated by MD simulations results shown in figure S19 going from ***t*A-GNP** to ***c*A-GNP**) makes ET less favored.

If excited state lifetime of the donor (τ_0) and the ET rate constant k_{ET} are considered, η_{ET} can be expressed as:

$$\eta_{ET} = \frac{1}{1 + \frac{k_{ET}}{\tau_0}}$$

[Eq. 12]

According to Eq. 12, for the same k_{ET}, ET efficiency is lower for shorter τ_0. *Cis* AB derivatives have been reported to show much shorter $\tau_0$than *trans* AB isomers.[14]

We would like to stress that these considerations about ET, that partially justify the different behavior of ***t*A-GNP** and ***c*A-GNP**, are only qualitative and that ultrafast transient absorption experiments are in due course to investigate ET in detail.

10. REFERENCES

[1] J. Kim, B. M. Novak, A. J. Waddon, *Macromolecules* **2004**, *37*, 8286-8292.
[2] F. Manea, C. Bindoli, S. Polizzi, L. Lay, P. Scrimin, *Langmuir* **2008**, *24*, 4120-4124.
[3] a) N. K. Chaki, Y. Negishi, H. Tsunoyama, Y. Shichibu, T. Tsukuda, *J. Am. Chem. Soc.* **2008**, *130*, 8608-+; b) H. Qian, R. Jin, *Nano Lett.* **2009**, *9*, 4083-4087.
[4] L. M. Tvedte, C. J. Ackerson, *J. Phys. Chem. A* **2014**, *118*, 8124-8128.
[5] M. Montalti, A. Credi, L. Prodi, M. T. Gandolfi, *Handbook of photochemistry*, CRC press, **2006**.
[6] G. Zimmerman, L.-Y. Chow, U.-J. Paik, *J. Am. Chem. Soc.* **1958**, *80*, 3528-3531.
[7] E. Pohjolainen, X. Chen, S. Malola, G. Groenhof, H. Häkkinen, *J. Chem. Theory Comput.* **2016**, *12*, 1342-1350.
[8] J. Wang, R. M. Wolf, J. W. Caldwell, P. A. Kollman, D. A. Case, *J. Comput. Chem.* **2004**, *25*, 1157-1174.
[9] C. I. Bayly, P. Cieplak, W. Cornell, P. A. Kollman, *J. Phys. Chem.* **1993**, *97*, 10269-10280.
[10] P. Duchstein, C. Neiss, A. Görling, D. Zahn, *J. Mol. Model.* **2012**, *18*, 2479-2482.
[11] O. Lopez-Acevedo, J. Akola, R. L. Whetten, H. Grönbeck, H. Häkkinen, *J. Phys. Chem. C* **2009**, *113*, 5035-5038.
[12] https://wiki.aalto.fi/display/CSM/Coordinates.
[13] a) T. L. Jennings, M. P. Singh, G. F. Strouse, *J. Am. Chem. Soc.* **2006**, *128*, 5462-5467; b) A. Samanta, Y. D. Zhou, S. L. Zou, H. Yan, Y. Liu, *Nano Lett.* **2014**, *14*, 5052-5057.
[14] H. M. D. Bandara, S. C. Burdette, *Chem. Soc. Rev.* **2012**, *41*, 1809-1825.